Optics Letters

Nonreciprocal strong mechanical squeezing based on the Sagnac effect and two-tone driving

Bo Zhao,[1,2] Ke-Xin Zhou,[1,2] Mei-Rong Wei,[1,2] Jinke Cao,[1,2] and Qi Guo[1,2,*]

[1]College of Physics and Electronic Engineering, Shanxi University, Taiyuan, Shanxi 030006, China
[2]Collaborative Innovation Center of Extreme Optics, Shanxi University, Taiyuan, Shanxi 030006, China
*qguo@sxu.edu.cn

Received 26 October 2023; revised 2 December 2023; accepted 18 December 2023; posted 19 December 2023; published 16 January 2024

We propose a scheme for generating nonreciprocal strong mechanical squeezing by using two-tone lasers to drive a spinning optomechanical system. For given driving frequencies, strong mechanical squeezing of the breathing mode in the spinning resonator can be achieved in a chosen driving direction but not in the other. The nonreciprocity originates from the Sagnac effect caused by the resonator's spinning. We also find the classical nonreciprocity and the quantum nonreciprocity can be switched by simply changing the angular velocity of the spinning resonator. We show that the scheme is robust to the system's dissipations and the mechanical thermal noise. This work may be meaningful for the study of nonreciprocal device and quantum precision measurement.

https://doi.org/10.1364/OL.510053

Mechanical squeezing is one of the most significant quantum effects, which plays an important part in quantum precision measurements [1–3] and quantum information processing [4–6]. The generation of mechanical squeezing has been an important goal in these fields. Many schemes have been proposed to achieve mechanical squeezing [4–16]. Especially, by using the reservoir engineering technique based on two-tone driving, the generation of the strong mechanical squeezing (exceeding the 3-dB limit [17]) has been realized in both theory [18] and experiment [19].

On the other hand, nonreciprocal physics has attracted intense attention due to its applications in signal transfer, communication, and the manipulation of light–matter interactions [20–23]. If a system behaves differently before and after exchanging the input and output directions, the system is nonreciprocal. By using light-atom coupling [24,25], synthetic materials [26,27], and optical nonlinearity [28–31] to break the Lorentz reciprocity, classical nonreciprocal effects have been achieved. Recently, quantum nonreciprocal effects have also been discussed, e.g., nonreciprocal photon blockade [32–35], nonreciprocal entanglement [36–38], nonreciprocal mechanical squeezing [39,40], and so on.

Motivated by these works above, in this Letter, we present a scheme to realize nonreciprocal strong mechanical squeezing in a spinning cavity optomechanical system driven by two-tone lasers. Moreover, we find one can switch the classical nonreciprocity (one-way flow of classical information, i.e., intracavity mean photon number) and the quantum nonreciprocity (nonreciprocal mechanical squeezing) by tuning the angular velocity of the spinning resonator. We also demonstrate the system's robustness to mechanical thermal noise. Compared with the existing schemes for nonreciprocal mechanical squeezing in Ref. [39,40], the presented scheme can realize the nonreciprocal *strong* mechanical squeezing (the degree of squeezing exceeds 3-dB limit) by using the simpler and more feasible experimental setup, and reveals the switch of the nonreciprocity between classical regime and quantum regime.

The system we considered is depicted in Fig. 1(a). It consists of a spinning resonator with angular velocity Ω and two parallel tapered fibers, and the spinning resonator is coupled with tapered fibers through evanescent fields. The clockwise (CW) or counterclockwise (CCW) mode of the resonator is driven by two-tone lasers (with mean frequency ω_l and detuning $\Delta_c \equiv \omega_c - \omega_l$) fed into fibers along the dashed lines or the solid lines. The optical Sagnac effect induced by the resonator's rotation is characterized by the Sagnac–Fizeau shift, i. e., $\omega_c \to \omega_c + \Delta_F$, with [41]

$$\Delta_F = \pm\Omega\frac{nR\omega_c}{c}\left(1 - \frac{1}{n^2} - \frac{\lambda}{n}\frac{dn}{d\lambda}\right), \tag{1}$$

where n (R) is the refractive index (radius) of the resonator, c (λ) is the speed (wavelength) of light in the vacuum, and $dn/d\lambda$ is the dispersion term. The dispersion term characterizes the relativistic origin of the Sagnac effect and can usually be ignored because it is small in typical materials [41,42]. For the resonator spinning clockwise, $\Delta_F > 0$ and $\Delta_F < 0$ refer to the shift of the CCW and the CW modes of the resonator, respectively. When the driving lasers are fed into fibers from the CCW direction, the Hamiltonian of the system is

$$\begin{aligned}\hat{H} &= \hbar\omega_L\hat{a}_L^\dagger\hat{a}_L + \hbar\omega_m\hat{b}^\dagger\hat{b} - \hbar g_0\hat{a}_L^\dagger\hat{a}_L(\hat{b}^\dagger + \hat{b}) + \hat{H}_{dr},\\ \hat{H}_{dr} &= \hbar(\alpha_+ e^{-i\omega_+ t} + \alpha_- e^{-i\omega_- t})\hat{a}_L^\dagger + \text{H.c.},\end{aligned} \tag{2}$$

where $\omega_{L(R)} \equiv \omega_c \pm |\Delta_F|$ and ω_m are the frequencies of CCW (CW) cavity mode and the mechanical mode, respectively. $\hat{a}_{L(R)}(\hat{b})$ is the photon (phonon) annihilation operator. $g_0 = (\omega_c/R) \times \sqrt{\hbar/2m\omega_m}$ denotes the single-photon cavity optomechanical coupling strength, with m is the mass of the resonator. $\omega_\pm$ and $\alpha_\pm$ are the frequency and amplitude of the two lasers.

Applying displacement transformation $\hat{a}_j = \overline{a}_{j+}e^{-i\omega_+ t} + \overline{a}_{j-}e^{-i\omega_- t} + \hat{d}_j$ ($j = L, R$) and $\hat{b} = \overline{b} + \delta\hat{b}$, in which $\overline{a}_{j\pm}$ is the coherent light field amplitude due to the two lasers. In order to drive the

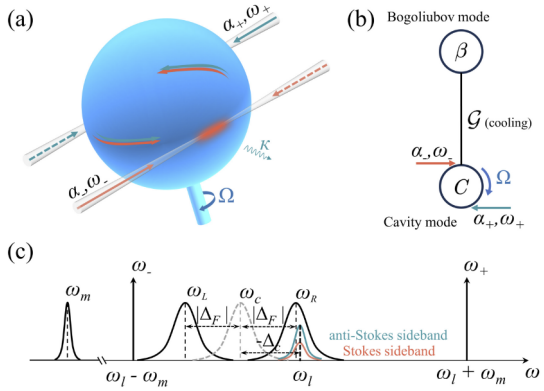

Fig. 1. (a) Schematic of the spinning optomechanical system. A resonator spinning clockwise is transitorily coupled with two parallel tapered fibers. Two-tone lasers enter the fibers along the dashed (solid) lines to drive the CCW (CW) mode. (b) Theoretical model for cooling the Bogoliubov mode using the cavity mode. (c) Frequency spectrum of the system for generating mechanical squeezing by CCW driving but not CW driving.

mechanical sidebands of the mean frequency $\omega_l = (\omega_+ + \omega_-)/2$, we choose the frequency $\omega_\pm = \omega_l \pm \omega_m$ [18]. The linearized Hamiltonian in the frame of $\hat{H}_0 = \hbar\omega_l \hat{d}_L^\dagger \hat{d}_L + \hbar\omega_m \delta\hat{b}^\dagger \delta\hat{b}$ is

$$\begin{aligned}\hat{H}_{\rm lin} =& -\hbar G_+(\hat{d}_L^\dagger \delta\hat{b}^\dagger + e^{-2i\omega_m t}\hat{d}_L^\dagger \delta\hat{b} + \text{H.c.}) \\ &- \hbar G_-(\hat{d}_L^\dagger \delta\hat{b} + e^{2i\omega_m t}\hat{d}_L^\dagger \delta\hat{b}^\dagger + \text{H.c.}) + \hbar\Delta_L \hat{d}_L^\dagger \hat{d}_L,\end{aligned} \tag{3}$$

where $\Delta_L = \omega_L - \omega_l = \omega_c \pm |\Delta_F| - \omega_l$ is the effective optical detuning (ignoring $g_0(\bar{b}^\dagger + \bar{b})$ because of $\omega_L/(\bar{b}^\dagger + \bar{b}) \gg g_0$). $G_\pm = g_0\bar{a}_{L\pm}$ are the enhanced optomechanical coupling strengths, where $G_\pm > 0$ and $\bar{a}_{L\pm} \gg 1$ [18,43–46].

For $G_\pm \ll \omega_m$, we can perform the rotating wave approximation (RWA), and the Hamiltonian is given by

$$\begin{aligned}\hat{H}_{\rm RWA} =& -\hbar G_+(\hat{d}_L^\dagger \delta\hat{b}^\dagger + \delta\hat{b}\hat{d}_L) \\ &- \hbar G_-(\hat{d}_L^\dagger \delta\hat{b} + \delta\hat{b}^\dagger \hat{d}_L) + \hbar\Delta_L \hat{d}_L^\dagger \hat{d}_L.\end{aligned} \tag{4}$$

By introducing a Bogoliubov-mode annihilation operator $\hat{\beta} = \hat{b}\cosh r + \hat{b}^\dagger \sinh r$, where r is the squeezing parameter defined *via* $\tanh r = G_+/G_-$, Eq. (4) can be written as $\hat{H} = -\hbar\mathcal{G}(\hat{d}_L^\dagger \hat{\beta} + \hat{d}_L \hat{\beta}^\dagger) + \hbar\Delta_L \hat{d}_L^\dagger \hat{d}_L$, where $\mathcal{G} = \sqrt{G_-^2 - G_+^2}$ denotes the coupling strength between CCW mode and Bogoliubov-mode. $G_+ < G_-$ is required to ensure the dynamics is stable [18,43–46]. CCW mode and Bogoliubov-mode are coupled by the beam splitter interaction [47,48], so the cavity can cool $\hat{\beta}$ mode, as shown in Fig. 1(b). Therefore, the mechanical squeezing can be obtained by cooling $\hat{\beta}$ mode to its ground state.

When the dissipation and input noises are considered, the quantum Langevin equations of the system can be obtained [49]

$$\begin{aligned}\dot{\hat{d}}_L =& i\left(G_+\delta\hat{b}^\dagger + G_-\delta\hat{b} - \Delta_L\hat{d}_L\right) - \frac{\kappa}{2}\hat{d}_L + \sqrt{\kappa}\hat{d}_L^{\rm in}, \\ \dot{\delta\hat{b}} =& i(G_+\hat{d}_L^\dagger + G_-\hat{d}_L) - \frac{\gamma_m}{2}\delta\hat{b} + \sqrt{\gamma_m}\hat{b}^{\rm in}.\end{aligned} \tag{5}$$

For the case without RWA, G_+ and G_- in Eq. (5) need to be replaced with $G_+ + G_- e^{2i\omega_m t}$ and $G_- + G_+ e^{-2i\omega_m t}$, respectively. Here, $\kappa(\gamma_m)$ is the cavity(mechanical) decay rate, and $\hat{d}_j^{\rm in}(\hat{b}^{\rm in})$ is the zero-mean input noise operator for the optical(mechanical) mode, respectively, characterized by the following correlation functions [49]: $\langle \hat{d}_j^{\rm in}(t)\hat{d}_j^{\rm in\dagger}(t')\rangle = \delta(t-t')$, $\langle \hat{b}^{\rm in}(t)\hat{b}^{\rm in\dagger}(t')\rangle = (n_{\rm th}+1)\delta(t-t')$, where $n_{\rm th} = [\exp(\hbar\omega_m/k_B T) - 1]^{-1}$ is the mean thermal phonon number, k_B is the Boltzmann constant, and T is the environmental temperature. By introducing quadrature operators

$$\begin{aligned}\delta\hat{Q} &= \frac{1}{\sqrt{2}}(\delta\hat{b}^\dagger + \delta\hat{b}), \quad \delta\hat{P} = \frac{i}{\sqrt{2}}(\delta\hat{b}^\dagger - \delta\hat{b}), \\ \hat{Q}^{\rm in} &= \frac{1}{\sqrt{2}}(\hat{b}^{\rm in\dagger} + \hat{b}^{\rm in}), \quad \hat{P}^{\rm in} = \frac{i}{\sqrt{2}}(\hat{b}^{\rm in\dagger} - \hat{b}^{\rm in}), \\ \delta\hat{X}_j &= \frac{1}{\sqrt{2}}(\hat{d}_j^\dagger + \hat{d}_j), \quad \delta\hat{Y}_j = \frac{i}{\sqrt{2}}(\hat{d}_j^\dagger - \hat{d}_j), \\ \hat{X}_j^{\rm in} &= \frac{1}{\sqrt{2}}(\hat{d}_j^{\rm in\dagger} + \hat{d}_j^{\rm in}), \quad \hat{Y}_j^{\rm in} = \frac{i}{\sqrt{2}}(\hat{d}_j^{\rm in\dagger} - \hat{d}_j^{\rm in}),\end{aligned} \tag{6}$$

and defining the column vectors of quadrature fluctuations and input noises as $u^T = (\delta\hat{Q}, \delta\hat{P}, \delta\hat{X}_L, \delta\hat{Y}_L)$, $v^T = (\sqrt{\gamma_m}\hat{Q}^{\rm in}, \sqrt{\gamma_m}\hat{P}^{\rm in}, \sqrt{\kappa}\hat{X}_L^{\rm in}, \sqrt{\kappa}\hat{Y}_L^{\rm in})$, we can rewrite the quantum Langevin equations as $\dot{u}(t) = Au(t) + v(t)$, where

$$A = \begin{pmatrix} -\frac{\gamma_m}{2} & 0 & 0 & G_+ - G_- \\ 0 & -\frac{\gamma_m}{2} & G_+ + G_- & 0 \\ 0 & G_+ - G_- & -\frac{\kappa}{2} & \Delta_L \\ G_+ + G_- & 0 & -\Delta_L & -\frac{\kappa}{2} \end{pmatrix}. \tag{7}$$

For the case without RWA, some maxtrix elements in Eq. (7) should be replaced: $A(1,3) = -A(4,2) = -(G_+ + G_-)\sin(2\omega_m t)$, $A(1,4) = A(3,2) = (G_+ - G_-)(1 - \cos(2\omega_m t))$, $A(2,3) = A(4,1) = (G_+ + G_-)(1 + \cos(2\omega_m t))$, $A(2,4) = -A(3,1) = -(G_+ - G_-)\sin(2\omega_m t)$, and all eigenvalues of A have a negative real part to ensure the system stability according to the Routh–Hurwitz criterion [50]. Due to the linearized dynamics of the quantum fluctuations and the zero-mean Gaussian nature of the quantum noises, the system will evolve into a Gaussian state independent of the initial states [51], and can be completely described by the 4×4 covariance matrix $V(t)$ with elements defined as $V_{kl} = \langle u_k(\infty)u_l(\infty) + u_l(\infty)u_k(\infty)\rangle/2$. Then we can derive the motion equation of the covariance matrix:

$$\dot{V}(t) = A(t)V(t) + V(t)A^T(t) + D, \tag{8}$$

where the diffusion matrix $D = \text{Diag}[(n_{\rm th} + 1/2)\gamma_m, (n_{\rm th} + 1/2)\gamma_m, \kappa/2, \kappa/2, \kappa/2, \kappa/2]$. For the steady state, Eq. (8) becomes the Lyapunov equation [52]:

$$AV + VA^T = -D. \tag{9}$$

By solving Eq. (8) and Eq. (9), we can get the time-dependent position variance and steady-state position variance of the mechanical mode, respectively.

From the derivation procedure above, one can see the ratio of coupling strengths G_+/G_- plays an important role, so we first plot the steady-state position variance $\langle\delta\hat{Q}^2\rangle$ for a stationary resonator ($\Omega = 0$ Hz) versus G_+/G_- in Fig. 2(a), which shows there is an optimal value for G_+/G_-, and the optimal values are not the same for different Δ_c. That is because the larger G_+/G_- the larger squeezing parameter r that leads to the decrease of the position variance. However, when $G_+/G_- \to 1$, $\mathcal{G} = \sqrt{G_-^2 - G_+^2} \to 0$, means the cooling ability is suppressed and the position variance will be increased. In Fig. 2(a), we choose experimentally feasible parameters [53–57]:

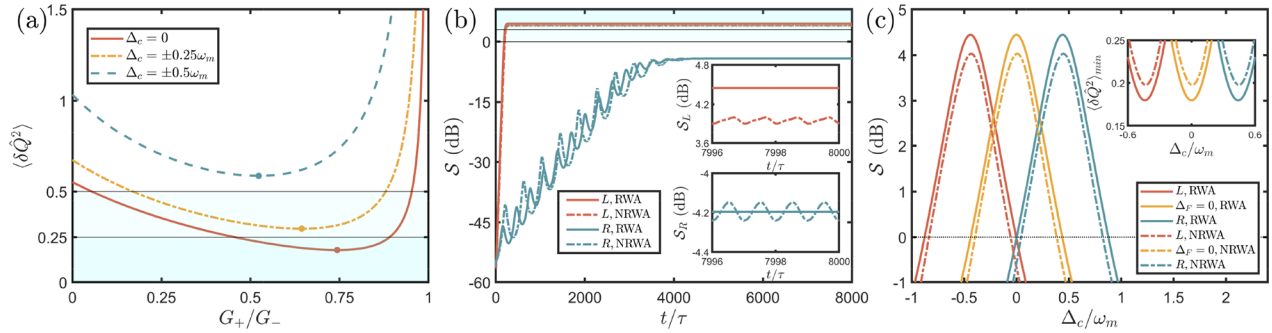

Fig. 2. (a) The steady-state position variance $\langle \delta\hat{Q}^2 \rangle$ versus G_+/G_-. $\Omega = 0$ Hz. See text for other parameters. (b) The time evolution of the degree of mechanical squeezing $\mathcal{S}$ without rotating wave approximation (NRWA) and with rotating wave approximation (RWA). $\mathcal{L}$ and $\mathcal{R}$ denote driving the resonator from the CCW and CW direction, respectively. $\tau = \pi/\omega_m$. $\Delta_c \equiv \omega_c - \omega_l = -|\Delta_F|$, $\Omega = 7.7$ kHz. The other parameters are the same as in (a). (c) $\mathcal{S}$ versus Δ_c/ω_m for different driving directions. The parameters are the same as in (b).

$n = 1.48$, $R = 1.1 \times 10^{-3}$ m, $T = 130$ mK, $\omega_m = 63 \times 10^6$ Hz, $\gamma_m = 0.5$ kHz, $\omega_c = 1.22 \times 10^{15}$ Hz, $\kappa = 0.3\,\omega_m$, and $G_- = 0.2\,\kappa$.

Figure 2(b) shows the dynamics of the degree of mechanical squeezing for the spinning resonator driven by two-tone lasers along CCW and CW directions, where the frequencies of two-tone lasers are chosen to satisfy $\Delta_c \equiv \omega_c - \omega_l = -|\Delta_F|$, as shown in Fig. 1(c). The degree of squeezing is defined in units of dB $\mathcal{S} = -10 \log_{10} \frac{\langle \delta\hat{Q}^2 \rangle_{\min}}{\langle \delta\hat{Q}^2 \rangle_{\rm vac}}$, where $\langle \delta\hat{Q}^2 \rangle_{\min}$ is the position variance corresponding to the optimal G_+/G_-, and $\langle \hat{Q}^2 \rangle_{\rm vac} = \frac{1}{2}$ is the vacuum quantum fluctuation. It can be seen that, for the given driving frequencies, the mechanical squeezing can only be generated by CCW driving but not CW driving. For exhibiting the nonreciprocal mechanical squeezing more clearly, we plot the steady-state degree of squeezing $\mathcal{S}$ for $t = 6000\tau$ versus Δ_c/ω_m in Fig. 2(c), which shows, for $\Delta_c < 0$, mechanical squeezing can be generated by driving the resonator from the CCW direction but not from the CW direction; while for $\Delta_c > 0$, the opposite is true. Meanwhile, the degree of squeezing exceeds 3-dB limit, so the nonreciprocal strong mechanical squeezing can be achieved. The inset of Fig. 2(c) shows the position variance corresponding to $\mathcal{S}$. The dot-dashed (solid) lines in both Figs. 2(b) and 2(c) indicate the results obtained without (with) RWA. The two results obtained using the Hamiltonians Eq. (3) and Eq. (4) agree well with each other, indicating that the RWA is valid [58].

We now study the classical nonreciprocal effect in the presented system by calculating the intracavity photon number of the driven mode and explore the relation between the classical nonreciprocity and the quantum nonreciprocity. The intracavity photon number of the driven mode is $N_j \equiv |\overline{a}_j|^2$. We can obtain the coherent light field amplitude $\overline{a}_j \simeq \overline{a}_{j+} e^{-i\omega_+ t} + \overline{a}_{j-} e^{-i\omega_- t}$ from quantum Langevin equations [43–45,59], where $\overline{a}_{j\pm} = \alpha_\pm/(\omega_\pm - \omega_j + i\frac{\kappa}{2})$, $|\alpha_\pm| = \sqrt{2\kappa P_\pm/\hbar\omega_\pm}$, and we assume $\overline{a}_{j\pm}$ are real by choosing the proper phases of the driving fields. $P_\pm$ is the input laser power. We plot the steady-state degree of squeezing $\mathcal{S}$ and intracavity photon number of the driven mode N_j as a function of Δ_c/ω_m in Fig. 3 with $P_- = 0.95$ mW, and P_+ is determined by P_- and the optimal G_+/G_-. The angular velocity of the spinning resonator $\Omega = 7.38$ kHz for Fig. 3(a), and $\Omega = 6.3$ kHz for Fig. 3(b). For $\Delta_c/\omega_m \sim -0.82$, when $\Omega = 7.38$ kHz, the quantum nonreciprocity exits without any classical nonreciprocity; however, when $\Omega = 6.3$ kHz, the classical nonreciprocity exits while the quantum nonreciprocity is absent. It means we can switch the quantum nonreciprocity and the classical nonreciprocity for

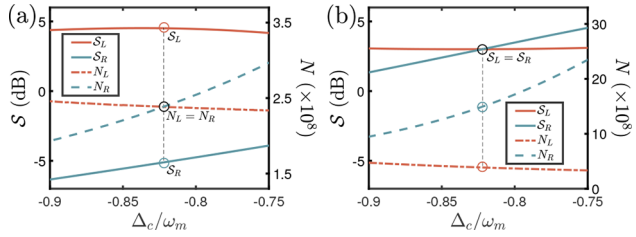

Fig. 3. Switch between the quantum nonreciprocity and the classical nonreciprocity. (a) Nonreciprocal strong mechanical squeezing exists with classical reciprocal intracavity photon number for $\Omega = 7.38$ kHz. (b) Classical nonreciprocal intracavity photon number exists with reciprocal strong mechanical squeezing for $\Omega = 6.3$ kHz. $m = 10ng$, $P_- = 0.95$ mW, and the other parameters are the same as in Fig. 2(c).

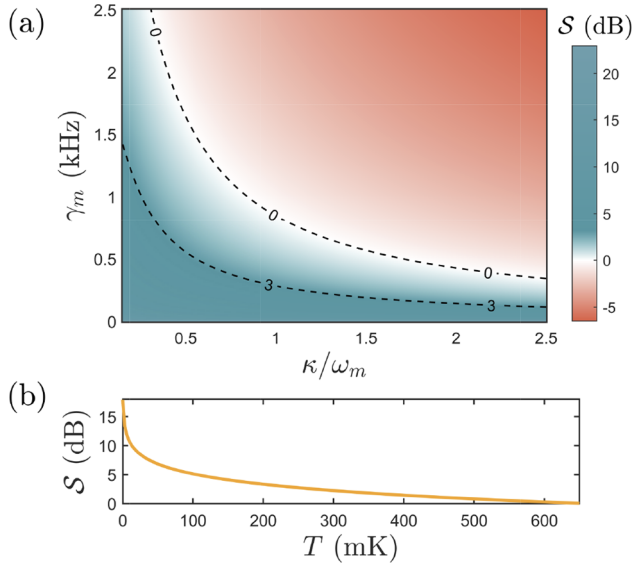

Fig. 4. (a) Steady-state degree of squeezing $\mathcal{S}$ versus the decay rates κ/ω_m and γ_m for $T = 130$ mK; The black dash lines indicate $\mathcal{S} = 0$ and 3 dB. (b) $\mathcal{S}$ versus the temperature T for $\kappa/\omega_m = 0.3$ and $\gamma_m = 0.5$ kHz. $\Omega = 0$ Hz, $\Delta_c/\omega_m = 0$ and the other parameters are the same as in Fig. 2(c).

a single device by simply tuning the angular velocity of the spinning resonator.

The robustness of the scheme against dissipations of the system and the environment temperature is demonstrated in Fig. 4. We plot the steady-state degree of squeezing $\mathcal{S}$ versus the decay rates κ/ω_m and γ_m at temperature $T = 130$ mK in Fig. 4(a), and versus the temperature for $\kappa/\omega_m = 0.3$ and $\gamma_m = 0.5$ kHz in Fig. 4(b). It shows that the squeezing and even the strong squeezing are present for a wide range of both κ and γ_m, and the squeezing can be still achieved even for $T \sim 650$ mK.

In conclusion, we have proposed a scheme to realize the nonreciprocal strong mechanical squeezing in a spinning cavity optomechanical system driven by two-tone lasers. The results show that the strong mechanical squeezing only occurs when the two-tone lasers with given frequencies drive the resonator from one direction but not the other. The validity of the theoretical derivation is demonstrated by using the full Hamiltonian to numerically simulate the results. We show the presented system can serve as either a classical nonreciprocal device or a quantum nonreciprocal device by choosing the appropriate angular velocity of the spinning resonator. The scheme is robust against dissipations and environmental temperature, and all results are based on the feasible parameters in experiment. Therefore, this work may provide effective methods for the study of quantum or classical nonreciprocal device and direction-dependent quantum precision measurement.

Funding. National Natural Science Foundation of China (12274274).

Disclosures. The authors declare no conflicts of interest.

Data availability. Data underlying the results presented in this paper are not publicly available at this time but may be obtained from the authors upon reasonable request.

REFERENCES

1. C. M. Caves, K. S. Thorne, R. W. P. Drever, *et al.*, Rev. Mod. Phys. **52**, 341 (1980).
2. M. D. LaHaye, O. Buu, B. Camarota, *et al.*, Science **304**, 74 (2004).
3. A. Motazedifard, F. Bemani, M. H. Naderi, *et al.*, New J. Phys. **18**, 073040 (2016).
4. S. Mancini, D. Vitali, and P. Tombesi, Phys. Rev. Lett. **90**, 137901 (2003).
5. S. L. Braunstein and P. van Loock, Rev. Mod. Phys. **77**, 513 (2005).
6. S. G. Hofer, W. Wieczorek, M. Aspelmeyer, *et al.*, Phys. Rev. A **84**, 052327 (2011).
7. C.-H. Bai, D.-Y. Wang, S. Zhang, *et al.*, Ann. Phys. **531**, 1800271 (2019).
8. W.-J. Zhang, Y. Zhang, Q. Guo, *et al.*, Phys. Rev. A **104**, 053506 (2021).
9. J.-Q. Liao and C. K. Law, Phys. Rev. A **83**, 033820 (2011).
10. W. Gu, G.-X. Li, and Y. Yang, Phys. Rev. A **88**, 013835 (2013).
11. D.-Y. Wang, C.-H. Bai, H.-F. Wang, *et al.*, Sci. Rep. **6**, 38559 (2016).
12. S. Huang and A. Chen, Phys. Rev. A **103**, 023501 (2021).
13. L.-J. Feng, G.-W. Lin, L. Deng, *et al.*, Sci. Rep. **8**, 3513 (2018).
14. W.-J. Gu, Z. Yi, Y. Yan, *et al.*, Ann. Phys. **531**, 1800399 (2019).
15. A. Dehghani, B. Mojaveri, and M. Aryaie, Quantum Inf. Process. **21**, 45 (2022).
16. W.-J. Gu, Z. Yi, L.-H. Sun, *et al.*, Opt. Express **26**, 30773 (2018).
17. G. Milburn and D. Walls, Opt. Commun. **39**, 401 (1981).
18. A. Kronwald, F. Marquardt, and A. A. Clerk, Phys. Rev. A **88**, 063833 (2013).
19. C. U. Lei, A. J. Weinstein, J. Suh, *et al.*, Phys. Rev. Lett. **117**, 100801 (2016).
20. Y. Shoji and T. Mizumoto, Sci. Technol. Adv. Mater. **15**, 014602 (2014). PMID: 27877640.
21. D. L. Sounas and A. Alù, Nat. Photonics **11**, 774 (2017).
22. P. Lodahl, S. Mahmoodian, S. Stobbe, *et al.*, Nature **541**, 473 (2017).
23. C. Caloz, A. Alù, S. Tretyakov, *et al.*, Phys. Rev. Appl. **10**, 047001 (2018).
24. S. Zhang, Y. Hu, G. Lin, *et al.*, Nat. Photonics **12**, 744 (2018).
25. P. Yang, X. Xia, H. He, *et al.*, Phys. Rev. Lett. **123**, 233604 (2019).
26. K. Fang, J. Luo, A. Metelmann, *et al.*, Nat. Phys. **13**, 465 (2017).
27. Q. Zhong, S. Nelson, Ş. K. Özdemir, *et al.*, Opt. Lett. **44**, 5242 (2019).
28. Z. Shen, Y.-L. Zhang, Y. Chen, *et al.*, Nat. Photonics **10**, 657 (2016).
29. Q.-T. Cao, H. Wang, C.-H. Dong, *et al.*, Phys. Rev. Lett. **118**, 033901 (2017).
30. Q.-T. Cao, R. Liu, H. Wang, *et al.*, Nat. Commun. **11**, 1136 (2020).
31. K. Xia, F. Nori, and M. Xiao, Phys. Rev. Lett. **121**, 203602 (2018).
32. R. Huang, A. Miranowicz, J.-Q. Liao, *et al.*, Phys. Rev. Lett. **121**, 153601 (2018).
33. B. Li, R. Huang, X. Xu, *et al.*, Photonics Res. **7**, 630 (2019).
34. Y.-M. Liu, J. Cheng, H.-F. Wang, *et al.*, Opt. Express **31**, 12847 (2023).
35. W. S. Xue, H. Z. Shen, and X. X. Yi, Opt. Lett. **45**, 4424 (2020).
36. Y.-F. Jiao, S.-D. Zhang, Y.-L. Zhang, *et al.*, Phys. Rev. Lett. **125**, 143605 (2020).
37. Y.-F. Jiao, J.-X. Liu, Y. Li, *et al.*, Phys. Rev. Appl. **18**, 064008 (2022).
38. Y. L. Ren, Opt. Lett. **47**, 1125 (2022).
39. Q. Guo, K.-X. Zhou, C.-H. Bai, *et al.*, Phys. Rev. A **108**, 033515 (2023).
40. S.-S. Chen, S.-S. Meng, H. Deng, *et al.*, Ann. Phys. **533**, 2000343 (2021).
41. G. B. Malykin, Phys.-Usp. **43**, 1229 (2000).
42. J. Kim, M. C. Kuzyk, K. Han, *et al.*, Nat. Phys. **11**, 275 (2015).
43. Y.-D. Wang and A. A. Clerk, Phys. Rev. Lett. **110**, 253601 (2013).
44. H. Tan, G. Li, and P. Meystre, Phys. Rev. A **87**, 033829 (2013).
45. L. F. Buchmann and D. M. Stamper-Kurn, Phys. Rev. A **92**, 013851 (2015).
46. J. Li, G. Li, S. Zippilli, *et al.*, Phys. Rev. A **95**, 043819 (2017).
47. F. Marquardt, J. P. Chen, A. A. Clerk, *et al.*, Phys. Rev. Lett. **99**, 093902 (2007).
48. I. Wilson-Rae, N. Nooshi, W. Zwerger, *et al.*, Phys. Rev. Lett. **99**, 093901 (2007).
49. C. W. Gardiner and P. Zoller, *Quantum Noise* (Springer, 2000).
50. E. X. DeJesus and C. Kaufman, Phys. Rev. A **35**, 5288 (1987).
51. C. Weedbrook, S. Pirandola, R. García-Patrón, *et al.*, Rev. Mod. Phys. **84**, 621 (2012).
52. D. Vitali, S. Gigan, A. Ferreira, *et al.*, Phys. Rev. Lett. **98**, 030405 (2007).
53. G. C. Righini, Y. Dumeige, P. Féron, *et al.*, Riv. del Nuovo Cim. **34**, 435 (2011).
54. X. Mao, H. Yang, D. Long, *et al.*, Photonics Res. **10**, 2115 (2022).
55. S. Maayani, R. Dahan, Y. Kligerman, *et al.*, Nature **558**, 569 (2018).
56. Y. Chen, Y.-L. Zhang, Z. Shen, *et al.*, Phys. Rev. Lett. **126**, 123603 (2021).
57. J.-X. Liu, Y.-F. Jiao, Y. Li, *et al.*, Sci. China Phys. Mech. Astron. **66**, 230312 (2023).
58. A. Frisk Kockum, A. Miranowicz, S. De Liberato, *et al.*, Nat. Rev. Phys. **1**, 19 (2019).
59. R. Zhang, Y. Fang, Y.-Y. Wang, *et al.*, Phys. Rev. A **99**, 043805 (2019).